MicL, a new σ^E-dependent sRNA, combats envelope stress by repressing synthesis of Lpp, the major outer membrane lipoprotein

Monica S. Guo,[1,5] Taylor B. Updegrove,[2,5] Emily B. Gogol,[1,4] Svetlana A. Shabalina,[3] Carol A. Gross,[1,6] and Gisela Storz[2,6]

[1]Department of Microbiology and Immunology, University of California at San Francisco, San Francisco, California 94158, USA; [2]Cell Biology and Metabolism Program, Eunice Kennedy Shriver National Institutes of Health, Bethesda, Maryland 20892, USA; [3]National Center for Biotechnology Information, National Institutes of Health, Bethesda, Maryland 20894, USA

In enteric bacteria, the transcription factor σ^E maintains membrane homeostasis by inducing synthesis of proteins involved in membrane repair and two small regulatory RNAs (sRNAs) that down-regulate synthesis of abundant membrane porins. Here, we describe the discovery of a third σ^E-dependent sRNA, MicL (mRNA-interfering complementary RNA regulator of Lpp), transcribed from a promoter located within the coding sequence of the *cutC* gene. MicL is synthesized as a 308-nucleotide (nt) primary transcript that is processed to an 80-nt form. Both forms possess features typical of Hfq-binding sRNAs but surprisingly target only a single mRNA, which encodes the outer membrane lipoprotein Lpp, the most abundant protein of the cell. We show that the copper sensitivity phenotype previously ascribed to inactivation of the *cutC* gene is actually derived from the loss of MicL and elevated Lpp levels. This observation raises the possibility that other phenotypes currently attributed to protein defects are due to deficiencies in unappreciated regulatory RNAs. We also report that σ^E activity is sensitive to Lpp abundance and that MicL and Lpp comprise a new σ^E regulatory loop that opposes membrane stress. Together MicA, RybB, and MicL allow σ^E to repress the synthesis of all abundant outer membrane proteins in response to stress.

[*Keywords*: sRNA; Hfq; *cutC*; copper; outer membrane homeostasis; σ^E]

Supplemental material is available for this article.

Received April 13, 2014; revised version accepted June 17, 2014.

The outer membrane (OM) of Gram-negative bacteria is its first line of defense against the environment, as it is a barrier against antibiotics and other stresses (for review, see Nikaido 2003). The OM is a complex environment consisting of outer leaflet lipopolysaccharide (LPS), inner leaflet phospholipids, and proteins such as OM porins (OMPs) and lipoproteins (for review, see Narita and Tokuda 2010; Silhavy et al. 2010; Ricci and Silhavy 2012; Zhang et al. 2013). The major *Escherichia coli* lipoprotein Lpp resides in the OM and is the most abundant protein in the cell (~1 million copies), comprising 2% of its dry weight (Narita and Tokuda 2010; Li et al. 2014). Approximately a third of the Lpp pool is conjugated to the peptidoglycan layer, serving as a structural element that connects the OM to the peptidoglycan (Braun and Rehn 1969; Inouye et al. 1972), while the remainder exists, at least in part, as a surface-exposed form that can be recognized by antimicrobial peptides (Cowles et al. 2011; Chang et al. 2012). Since cells synthesize a new OM each cell cycle, OM components are synthesized and transported at a tremendous rate. Indeed, at 37°C, >5% of all active ribosomes are devoted to Lpp translation (Li et al. 2014). Therefore, balancing the massive flux of membrane components with sufficient transport and assembly factors is vital for OM homeostasis.

In *E. coli* and related γ-proteobacteria, OM homeostasis is monitored by the essential transcription factor σ^E, which responds to perturbations to OMP and LPS folding

[4]Present address: Genentech, Inc., South San Francisco, CA 94080, USA.
[5]These authors contributed equally to this work.
[6]Corresponding authors
E-mail storzg@mail.nih.gov
E-mail cgrossucsf@gmail.com
Article is online at http://www.genesdev.org/cgi/doi/10.1101/gad.243485.114.

(Walsh et al. 2003; Barchinger and Ades 2013; Lima et al. 2013; Zhang et al. 2013). σ^E activity is regulated by the degradation rate of its negative regulator, RseA, which holds σ^E inactive in the inner membrane. RseA cleavage is initiated by DegS in response to unfolded OMP stress, but a second regulator, RseB, binds to RseA and protects it from cleavage by DegS (Walsh et al. 2003; Chaba et al. 2011). Off-pathway LPS can bind to RseB and relieve its inhibition of DegS (Lima et al. 2013). Once RseA is cleaved, it undergoes proteolytic degradation and releases σ^E (Chaba et al. 2007). As σ^E activation is thus dependent on two signals, only concomitant OMP and LPS dysfunction will lead to maximal induction of σ^E (Lima et al. 2013).

Activation of σ^E induces expression of ~100 genes, including all of the machinery required for the transport and assembly of LPS and OMPs into the OM (Braun and Silhavy 2002; Wu et al. 2005; Rhodius et al. 2006; Skovierova et al. 2006). As the synthesis rate of new OM components is so high, increasing production of chaperones and transport factors may not be sufficient to rapidly restore folding during stress conditions. To combat this problem, σ^E additionally induces expression of two small regulatory RNAs (sRNAs), MicA and RybB, which act to inhibit synthesis of all major OMPs (Rasmussen et al. 2005; Udekwu et al. 2005; Johansen et al. 2006; Papenfort et al. 2006, 2010; Thompson et al. 2007; Udekwu and Wagner 2007).

sRNAs are integral to a myriad of bacterial stress responses, usually interacting with their *trans*-encoded target mRNAs via base-pairing to change message stability or translation (for review, see Richards and Vanderpool 2011; Storz et al. 2011). In enteric bacteria, these base-pairing sRNAs are associated with the RNA chaperone Hfq, which binds to and protects sRNAs from nuclease degradation and facilitates the intermolecular contacts between sRNAs and target mRNAs (for review, see Vogel and Luisi 2011). Only limited base-pairing is required for productive interaction. This inherent degeneracy in targeting sequences allows sRNAs to have multiple targets and, conversely, allows for specific mRNAs to have multiple sRNA regulators.

The σ^E-dependent sRNAs MicA and RybB bind to Hfq and together target 31 messages for degradation, including mRNAs encoding the major porins as well as proteins in metabolism, ribosomal biogenesis, a toxin anti-toxin system, and the transcriptional factor PhoP (Coornaert et al. 2010; Gogol et al. 2011). The promoters of MicA and RybB are the second and third strongest in the σ^E regulon, weaker than only the σ^E promoter itself (Mutalik et al. 2009). These sRNAs have strong protective effects on membrane homeostasis, as they can rescue cell death resulting from the membrane blebbing and lysis associated with loss of σ^E activity (Hayden and Ades 2008; Gogol et al. 2011), presumably by down-regulating *omp* mRNA and rebalancing the membrane (Papenfort et al. 2010; Gogol et al. 2011).

Here we report the discovery and characterization of a third σ^E-dependent sRNA and show that this sRNA is dedicated to the regulation of Lpp. We name this sRNA MicL for mRNA-interfering complementary RNA regulator of Lpp, following the nomenclature of Mizuno et al. (1984). MicL is transcribed from a strong σ^E-dependent promoter within the *cutC* coding sequence and subsequently processed into a smaller transcript (MicL-S). It is responsible for all phenotypes previously associated with loss of *cutC*. We discuss how our finding that MicL/Lpp constitute a novel regulatory loop modulating σ^E activity expands our view of the cellular mechanism for maintaining OM homeostasis as well as the implications of sRNAs evolving from the 3′ end of transcripts.

Results

MicL is a third σ^E-regulated sRNA

To identify novel σ^E-dependent sRNAs in *E. coli*, we used a tiled microarray to examine whole-genome expression after ectopic σ^E overexpression. Along with the previously identified σ^E-dependent sRNAs MicA and RybB, we observed two overlapping transcripts that were strongly up-regulated in a σ^E-dependent manner within the 3′ end of *cutC* and the intergenic region between *cutC* and *torY* (Fig. 1A). These transcripts are likely the same as RyeF, a putative sRNA previously identified in the *cutC*/*torY* intergenic region of *E. coli* and *Salmonella* (Zhang et al. 2003a; Chao et al. 2012). We did not observe a σ^E-dependent transcript upstream of *cutC*, suggesting that *cutC* itself is not σ^E-dependent (data not shown). Additionally, we did not observe the previously postulated σ^E regulation of CyaR (Johansen et al. 2008), suggesting that this sRNA is unlikely to be directly regulated by σ^E (data not shown).

Northern analysis of total RNA isolated from cells with and without ectopic expression of σ^E validated the presence of two σ^E-dependent transcripts, an ~300-nucleotide (nt) transcript denoted as MicL and an ~80-nt transcript denoted as MicL-S, which were detected with a probe to the 3′ end of *cutC* (Fig. 1B). Both MicL and MicL-S are induced during transition to stationary phase, a time when σ^E activity increases dramatically (Ades et al. 1999; Costanzo and Ades 2006). The two bands showed maximal expression during late stationary phase in defined rich medium (around ~15 h) (Fig. 1C) and in LB (data not shown), consistent with σ^E induction.

Primer extension and total mRNA sequencing (mRNA-seq) analysis revealed that the 308-nt MicL transcript begins within *cutC* (226 nt before the *cutC* stop codon) and ends at the *cutC* intrinsic terminator, significantly upstream of the start of *torY* (Supplemental Fig. S1A,B; data not shown). The 80-nt MicL-S begins with the last base of the *cutC* stop codon and ends at the *cutC* terminator. Thus, both forms of MicL contain the full *cutC* 3′ untranslated region (UTR).

We identified a putative σ^E promoter upstream of the start of MicL (P_{micL}) (Fig. 1D; Rhodius et al. 2006) but not in front of MicL-S. Strong conservation of this sequence within the *cutC* coding sequence is observed in *Shigella*, *Salmonella*, *Citrobacter*, *Klebsiella*, *Cronobacter*, and

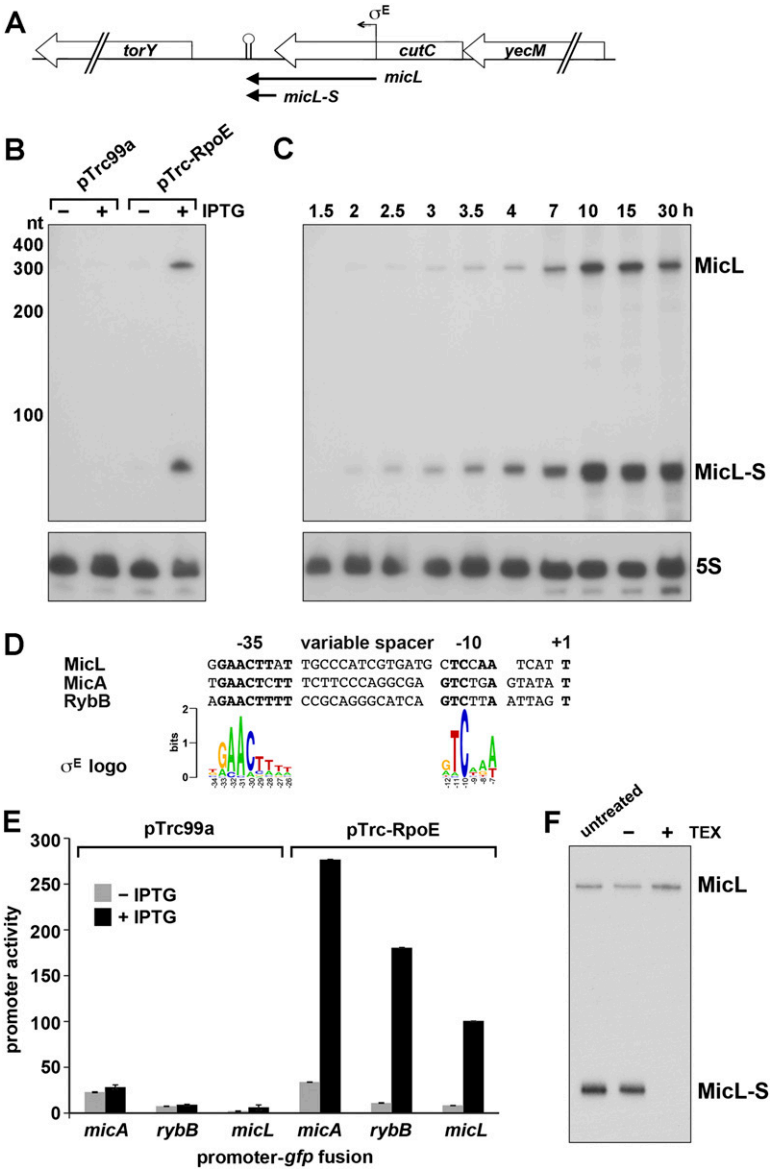

Figure 1. MicL expression is regulated by σ^E. (*A*) Schematic of the genomic context of MicL; its processed transcript, MicL-S; and *cutC* (see Supplemental Fig. S1B). (*B*) MicL levels increase following σ^E overexpression. Cells harboring either vector or a σ^E expression plasmid growing exponentially in EZ rich defined medium were induced with 1 mM IPTG for 1 h. RNA was extracted and probed for the 3′ end of MicL and 5S RNA. (*C*) MicL levels increase in stationary phase. Total RNA was extracted at the indicated times during growth in EZ rich defined medium and probed for MicL and 5S RNA. (*D*) The *micL* promoter is similar to a logo for σ^E promoter sequences (Rhodius et al. 2012). (*E*) P_{micL} is σ^E dependent. Cells carrying either the vector control or the pTrc-RpoE plasmid, expressing GFP from the indicated minimal promoters (−65 to +20 relative to transcription start site), and growing exponentially in LB were induced with 1 mM IPTG, and GFP fluorescence was monitored. Promoter activity was measured by normalizing GFP fluorescence by OD (see the Materials and Methods). (*F*) MicL-S is a processed transcript. RNA isolated following induction of MicL for 3 h from an IPTG-inducible promoter was left untreated, incubated in buffer, or incubated in buffer with 5′ monophosphate-dependent terminator exonuclease (TEX). MicL-S levels were subsequently probed.

Enterobacter species but not in more distantly related enteric bacteria (Supplemental Fig. S2A–D). A fusion of the minimal putative P_{micL} promoter (−65 to +20) to GFP is induced by ectopic σ^E overexpression and is only slightly weaker than the strong σ^E-dependent *micA* and *rybB* promoters in the same vector background (Fig. 1E). Together, these data show that MicL is a third σ^E-dependent sRNA in *E. coli* and likely in related enteric bacteria.

MicL-S is processed from MicL

MicL-S may be processed from MicL, as we did not observe a promoter for MicL-S. We tested this by treating total RNA with 5′ monophosphate-dependent terminator exonuclease (TEX), which degrades processed transcripts but spares primary transcripts, as they have 5′ triphosphates. Following TEX treatment, MicL-S is degraded, but the MicL level is virtually unchanged (Fig. 1F), suggesting that MicL-S is generated by ribonucleolytic cleavage of MicL.

We examined MicL levels after 15 min of MicL induction from P_{LacO-1} and subsequent IPTG washout (Supplemental Fig. S3A). The observations that MicL-S is detected only after induction of MicL and that MicL and MicL-S disappear with similar kinetics support the idea that MicL-S is derived from MicL. Importantly, MicL-S expressed independently from the P_{LacO-1} promoter has the same half-life as MicL-S cleaved from MicL (Supplemental Fig. S3B), demonstrating that cleavage does not impact MicL-S stability.

We next investigated the mechanism of MicL processing. Although the MicL cleavage site is within the *cutC* TGA stop codon, this sequence is not a cleavage signal, as a TGA-to-GGA mutation did not alter processing (Supplemental Fig. S3C). RNase E is the primary RNase in *E. coli* and mediates processing of other sRNAs (Massé et al.

2003), but production of MicL-S was not abolished in a *rne*-3071 mutant (Supplemental Fig. S3D) or in strains lacking various other RNases (Opdyke et al. 2011), including RNase III (*rnc*), RNase G (*rng*), RNase BN (*elaC*), five toxin endonucleases (Supplemental Fig. S3E), and the broadly conserved YbeY RNase (data not shown). Either uncharacterized ribonucleases mediate MicL processing or other combinations of RNases perform this function.

Lpp is the sole target of MicL

Transcripts from the 3′ UTR of *cutC* (RyeF) coimmunoprecipitate with Hfq in *E. coli* and *Salmonella* (Zhang et al. 2003a; Chao et al. 2012). We validated this observation for both MicL and MicL-S, which coimmunoprecipitate with Hfq at ratios consistent with their levels, suggesting that both forms bind Hfq with similar affinity (Fig. 2A). In addition, both MicL transcripts are virtually undetectable in strains lacking Hfq (*hfq-1*), indicating that their stabilities are Hfq-dependent (Fig. 2A).

Hfq-binding sRNAs in *E. coli* have all been found to regulate target mRNAs via limited base-pairing, enabling them to regulate expression of multiple targets. With this expectation, we searched for targets of MicL. However, analysis of mRNA-seq data taken before and after expression of MicL for 4, 10, and 20 min identified only a single MicL target, *lpp* (Fig. 2B; Supplemental Fig. S4A; Supplemental Table S1). The levels of *lpp* mRNA were reduced starting 4 min after induction and were down-regulated by 20-fold after 20 min (Supplemental Fig. S4C). The OM lipoprotein Lpp, the most abundant protein in the cell, is a key component of the membrane. σ^E was previously reported to repress *lpp* via an unknown mechanism that required Hfq (Rhodius et al. 2006; Guisbert et al. 2007). Stunningly, even after the 20-fold reduction in *lpp* mRNA due to MicL overexpression, *lpp* is still the 12th most abundant mRNA in the cell (Supplemental Table S1).

We examined the possibility that other MicL targets might be regulated solely at the level of translation by sequencing ribosome-protected mRNA fragments (ribosome profiling) (Ingolia et al. 2009) after ectopic expression of MicL at the same time points used above for mRNA-seq (Fig. 2C; Supplemental Table S2). Similar to what we observed for the steady-state mRNA levels, expression of MicL decreased translation of *lpp* ~10-fold after a 20-min induction of MicL. For all other transcripts, translation was not significantly altered by MicL overexpression (Supplemental Fig. S4E,F). *lpp* is the most well-translated mRNA in the cell and remains the 30th most well-translated mRNA after MicL expression (Supplemental Table S2). Together, these experiments strongly suggest that *lpp* is the sole MicL target under the conditions tested.

MicL repression of Lpp mimics lpp deletion phenotypes

Strains lacking Lpp were reported to be sensitive to membrane perturbants such as dibucaine, deoxycholate, sodium dodecyl sulfate (SDS), and ethylenediaminetetraacetic acid (EDTA) (Hirota et al. 1977; Suzuki et al. 1978; Nichols et al. 2011). Using the reported concentrations

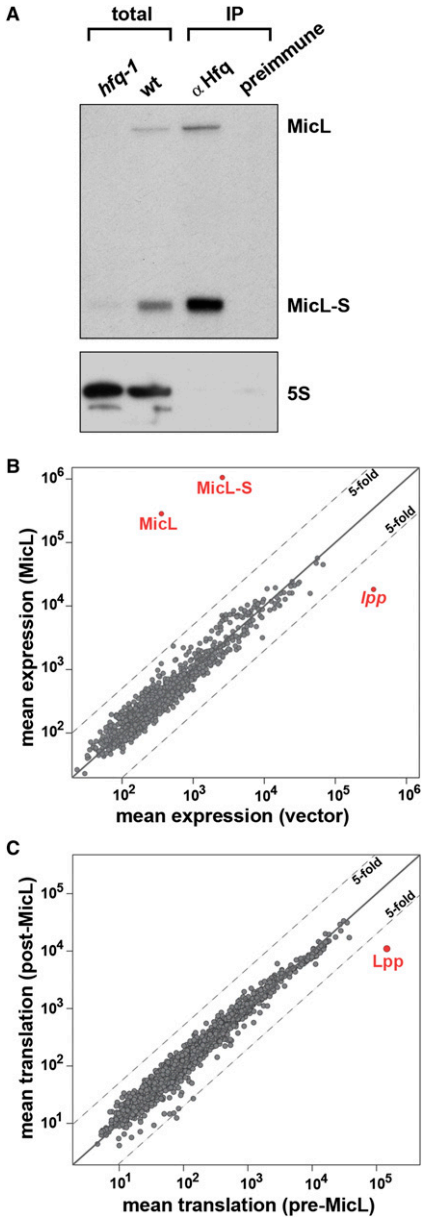

Figure 2. *lpp* is the sole target of MicL. (*A*) MicL interacts with Hfq. Extracts were prepared from wild-type cells after 16 h of growth in LB medium and subjected to immunoprecipitation with α-Hfq or preimmune serum. MicL was probed in the immunoprecipitated samples (0.5 μg of RNA loaded) as well as on total RNA isolated from wild-type and the isogenic *hfq-1* mutant cells (5 μg of RNA loaded). (*B*) MicL expression reduces *lpp* mRNA levels ~20-fold. mRNA-seq was performed in exponential phase after 20 min of MicL induction from pBR′-MicL at 30°C in EZ rich defined medium and compared with a similarly treated vector control strain. Expression level is in reads per kilobase per million (RPKM). (*C*) MicL expression reduces translation on *lpp* mRNA ~10-fold. Ribosome profiling was performed in exponential phase after 20 min of MicL induction from pBR′-MicL at 30°C in EZ rich defined medium and compared with profiles taken before MicL induction. Relative translation is in RPKM. Other genes (*fepA* and *fiu*) close to the fivefold cutoff are repressed by growth (Supplemental Fig. S4F).

for these chemicals, we found that dibucaine yielded the strongest distinction between wild-type and Δ*lpp* strains, with the latter having small, translucent colonies in the presence of dibucaine. (Fig. 3A). Cells harboring MicL or MicL-S appeared mildly translucent on dibucaine in the absence of inducer and become markedly translucent after addition of inducer (cf. Fig. 3A and Supplemental Fig. S5). Δ*lpp* cells additionally display a small (~10-fold) decrease in viability, but this was not observed for wild-type cells overexpressing either MicL or MicL-S, possibly because such cells still retain some Lpp. Overexpression of MicL or MicL-S in a Δ*lpp* background did not further sensitize cells to dibucaine (Fig. 3A), supporting the conclusion that the dibucaine sensitivity associated with MicL overexpression is due to decreased *lpp* levels.

Endogenous levels of MicL are sufficient to repress lpp

To determine whether MicL expressed from its native locus had the capacity to repress *lpp*, we assayed *lpp* mRNA levels upon σ^E overexpression. Indeed, elevated σ^E led to reduced *lpp* mRNA in wild-type cells but not in a strain lacking MicL (Δ*cutC*) (Fig. 3B). We also tested whether *lpp* mRNA was down-regulated in stationary phase when MicL levels are highest (Fig. 1C). As can be seen in Figure 3C, in stationary phase (10 or 15 h of growth), *lpp* transcript levels are less abundant in wild-type cells than in cells lacking MicL. We also observed higher accumulation of Lpp protein in the Δ*cutC* strain compared with the wild-type strain. The Lpp protein level does not mirror changes in *lpp* mRNA, as the protein is stable and therefore accumulates in stationary phase because proteins are no longer diluted by cell division. Interestingly, even in the Δ*cutC* strain, we saw a sharp decrease in *lpp* mRNA levels during stationary phase, suggesting the existence of additional regulators of *lpp* expression and highlighting the importance of reducing Lpp levels in stationary phase (Fig. 3C).

MicL-S base-pairs directly with lpp mRNA

To test for direct base-pairing between MicL and *lpp*, we generated a translational fusion by integrating the *lpp* 5′ UTR (containing sequences from the transcription start site through 102 nt of the *lpp* coding sequence) in-frame to the seventh codon of *lacZ* gene, all downstream from the heterologous P_{BAD} promoter in the chromosome of PM1205 (Mandin and Gottesman 2009). The β-galactosidase activity of this reporter strain was reduced more than twofold by ectopic overexpression of both MicL

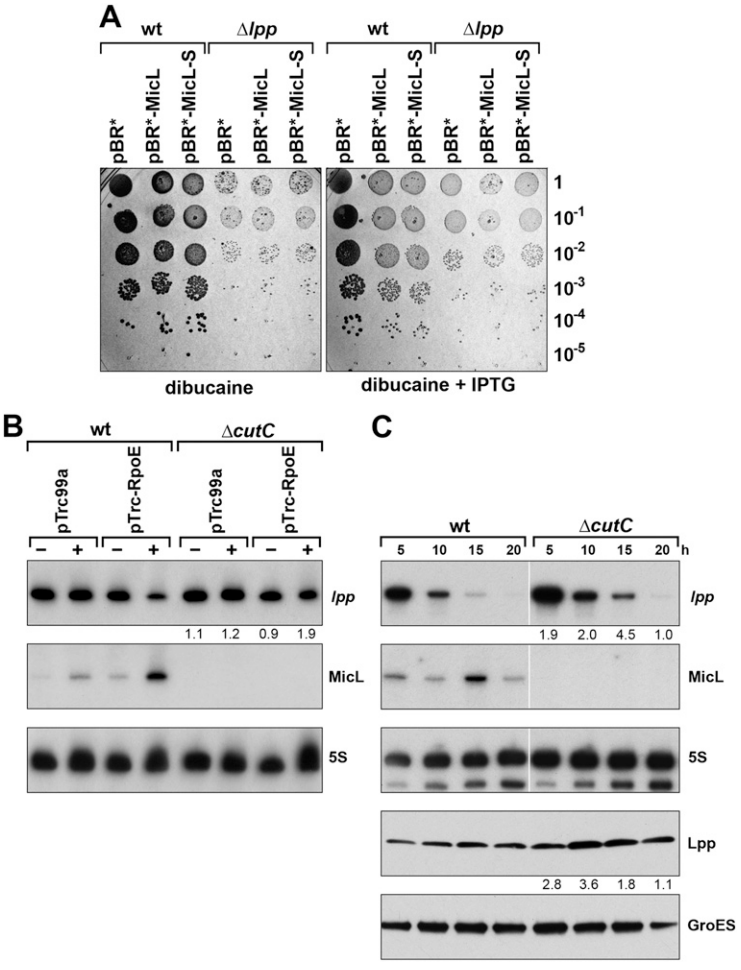

Figure 3. MicL repression of *lpp* is physiologically important. (*A*) Expression of MicL phenocopies the dibucaine sensitivity of Δ*lpp*. Wild-type or Δ*lpp* cells carrying pBR*-MicL, pBR*-MicL-S, or empty vector were spotted at the indicated dilutions on LB plates containing 1.4 mM dibucaine with or without 1 mM IPTG. (*B*) MicL represses *lpp* RNA levels following σ^E overexpression. Wild type and a Δ*cutC* strain with either control vector or pRpoE growing exponentially in LB (OD_{600} ~0.1) were induced with 1 mM IPTG for 2 h. Total RNA was isolated and probed for *lpp*, MicL, and 5S RNA. (*C*) *lpp* mRNA and Lpp protein levels in wild-type and Δ*cutC* mutant backgrounds. At the indicated times, total RNA was extracted from wild type and the Δ*cutC* mutant strain grown in LB. Total RNA was probed to examine *lpp*, MicL, and 5S RNA levels, and Lpp and GroEL protein levels were examined by immunoblotting protein samples taken at the same time points. For *B* and *C*, the intensity of the *lpp* RNA or protein band for each strain was quantified using ImageJ software, and the ratios between the corresponding samples for the Δ*cutC* mutant and wild-type strains are given.

and MicL-S but not by overexpression of MicA or RybB (Fig. 4A). As both forms of MicL down-regulate *lpp*, the region required for regulation must be within MicL-S. To further define the regulatory sequences, we tested whether 5′ truncations of MicL-S retained the ability to regulate the *lpp-lacZ* translational reporter. A MicL-S variant lacking the first 12 nt (MicL-SΔ1) fully repressed the fusion, while a MicL-S variant lacking the first 45 nt (MicL-SΔ2) did not, placing the sequence required for regulation between nucleotides +13 and 44 of MicL-S (Supplemental Fig. S6). We similarly defined the MicL-responsive region of *lpp*, finding that a truncation retaining the first 33 nt of the *lpp* coding sequence is repressed by MicL-S (*lppΔ2*), but a truncation that retains only the first 6 nt of the coding sequence is not (*lppΔ3*), suggesting that a portion of the sequence targeted by MicL lies between +6 and 33 nt of the *lpp* coding sequence (+43–70 nt from the start of the of *lpp* mRNA) (Supplemental Fig. S6).

Computational analysis of these regions using ThermoComposition software (Matveeva et al. 2007) also suggested possible base-pairing between +19 and 49 of MicL-S (Fig. 4B,C) and +16 and 46 of the *lpp* coding sequence. Indeed, MicL-S-1, harboring a 4-nt mutation in the predicted pairing region of MicL-S (altered nucleotides +41–44) (Fig. 4B,C), was unable to repress the *lpp-lacZ* reporter (Fig. 4D), but a compensatory mutation in *lpp* (*lpp-lacZ-1*, altered nucleotides +21–25 of the coding sequence) restored repression to levels comparable with wild-type regulation (Fig. 4D). We verified that MicL-S and MicL-S-1 accumulate to similar levels, and while MicL-S noticeably reduced *lpp* mRNA and Lpp protein levels, MicL-S-1 does not (Fig. 4E). Thus, MicL-S is an sRNA that directly base-pairs with and represses *lpp*.

Stable duplex predictions between *cutC* and *lpp* in various bacteria revealed that the extensive region of base-pairing—and particularly a stable core (seed) interaction between +38 and 49 of MicL-S and +16 and 28 of the *lpp* coding sequence—is conserved in only a select group of enteric bacteria, consistent with a recent evolution of the MicL RNA (Supplemental Figs. S2A–D, S7). Interestingly, while *Salmonella enterica* contains two *lpp* genes (*lppA* and *lppB*), the long stretch of MicL complementarity is detected for only one of the two *lpp* genes (*lppA*) found in this organism.

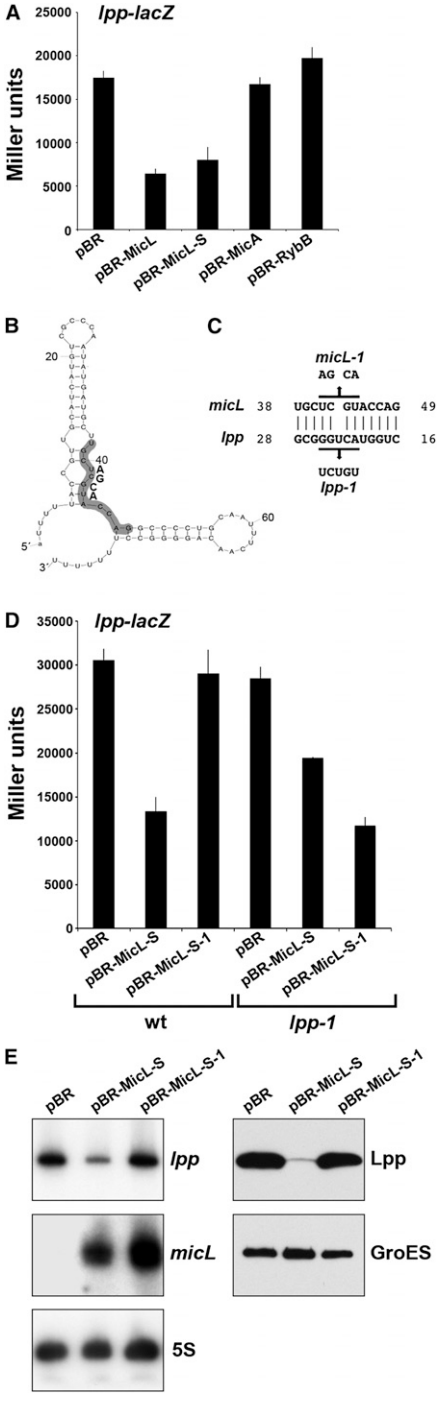

Figure 4. MicL base-pairs with *lpp*. (*A*) MicL and MicL-S, but not MicA and RybB, repress an *lpp-lacZ* translational fusion. β-Galactosidase activity of the *lpp-lacZ* fusion preceded by a P_{BAD} promoter was assayed in strains with control vector, pBR-MicL, pBR-MicL-S, pBR-MicA, and pBR-RybB plasmids after 3 h of induction with 0.2% arabinose (for fusion) and 1 mM IPTG (for sRNA) (final OD_{600} ~1.0) in LB. Average values and standard deviations from four independent experiments are shown. (*B*) Predicated structure of MicL-S. Nucleotides predicted to comprise the core of base-pairing with *lpp* are shaded. (*C*) Predicted MicL and *lpp* base-pairing core with mutations designed to disrupt interaction. (*D*) Effect of disruption and restoration of base-pairing on MicL repression of *lpp-lacZ*. Plasmids carrying wild-type MicL-S or the MicL-S-1 derivative were transformed into strains containing *lpp-lacZ* or *lpp-1-lacZ*, which carries compensatory mutations to restore base-pairing with MicL-S-1. β-Galactosidase activity was assayed as in *A*. (*E*) MicL-S but not MicL-S-1 lowers *lpp* RNA and Lpp protein levels. The *lpp-lacZ* fusion strain was transformed with pBR-MicL-S or pBR-MicL-S-1 and induced as in *A*. Samples were collected after 3 h, and levels of *lpp*, the MicL-S and 5S RNA, or the Lpp and GroEL proteins were probed.

MicL represses lpp by inhibiting translation

Most sRNAs inhibit translation by sterically occluding the Shine-Dalgarno sequence or the start codon, prevent-

ing ribosomes from accessing target mRNA (for review, see Desnoyers et al. 2013). As the core of MicL base-pairing with *lpp* is downstream from the translation start site (+16–28 nt of the *lpp* coding sequence) (Fig. 5A), at the edge of the region where sRNA binding is known to interfere with translation initiation (Bouvier et al. 2008), it is unclear whether MicL represses translation or affects mRNA stability independently of translation. To examine this, we tested whether MicL-S overexpression reduces the mRNA levels of *lpp* derivatives harboring early stop mutants (stop codon at the start and second and fourth codons) (Fig. 5A). While the *lpp* stop mutant at the start codon cannot be translated, translation should initiate for the other two derivatives. Although the absolute levels of *lpp* mRNA are altered, we no longer observed a significant decrease in *lpp* mRNA levels following MicL-S overexpression in any of these strains (Fig. 5B). This suggests that the primary effect of MicL is to inhibit translation of *lpp* rather than to mediate *lpp* mRNA degradation and that increased degradation is a consequence of the fact that untranslated mRNAs are not protected from ribonucleolytic cleavage (Nilsson et al. 1984).

Consistent with the idea that *lpp* mRNA is rapidly degraded in the absence of active translation, we observed that expression of MicL did not significantly decrease the translation efficiency (ribosomes per unit mRNA) of *lpp* (Fig. 5C). This suggests that every *lpp* mRNA is being translated by the same number of ribosomes regardless of the level of MicL. Thus, *lpp* mRNA either is undergoing active translation or is rapidly cleared when MicL binding blocks translation.

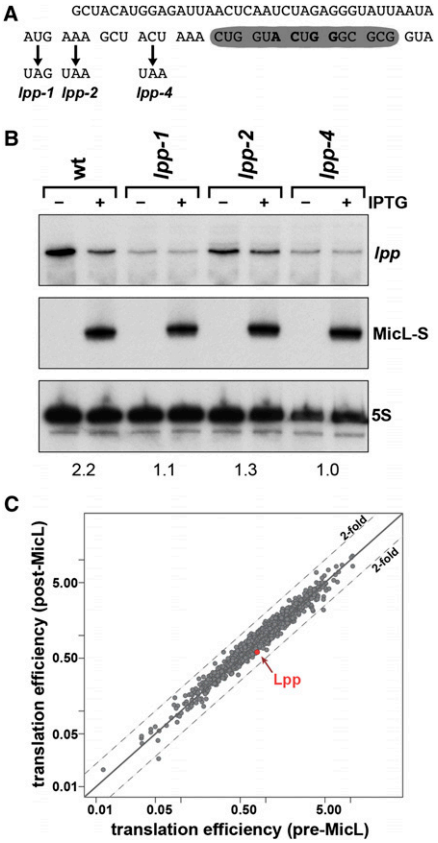

Figure 5. MicL repression of *lpp* is dependent on translation. (*A*) Diagrammatic representation of the derivatives carrying early stop codon mutations *lpp-1* (ATG to TAG at the first codon), *lpp-2* (AAA to TAA at the second codon), and *lpp-4* (ACT to TAA at the fourth codon). (*B*) The pBR*-MicL-S plasmid was transformed into wild-type and *lpp* translation-defective cells, MicL-S was induced with 1 mM IPTG in LB for 3 h, and RNA was extracted (final OD_{600} ~1.0) and probed for *lpp*, MicL-S, and 5S RNA. The intensity of the *lpp* band from each strain was quantified using ImageJ software, and the fold changes listed *below* are calculated for the corresponding samples with and without IPTG. Immunoblot analysis for Lpp confirmed that translation was eliminated in the stop codon mutants (data not shown). (*C*) Translation efficiency of Lpp is unchanged after MicL expression. Translation efficiency per gene after 20 min of MicL induction is plotted versus translation efficiency before MicL induction. Translation efficiency was calculated as the number of ribosome footprints per gene/mRNA reads per gene from the ribosome profiling and mRNA-seq data.

Phenotypes ascribed to ΔcutC are due to eliminating MicL repression of lpp

The *cutC* gene was reported to be involved in copper homeostasis because missense mutations in *cutC* alone and in combination with mutations in *nlpE* lead to copper sensitivity (Gupta et al. 1995). Interestingly, the *cutC* mutations leading to copper sensitivity are clustered around the P_{micL} promoter: One lies between the P_{micL} −10 and −35 motifs (nucleotide change G197A, amino acid change R66H), and the other is located at −67 from the P_{micL} start (nucleotide change A146G, amino acid change K49R), raising the possibility that the copper phenotype of *cutC* could be due to misregulation of MicL. We tested this possibility by determining the copper phenotype of two constructs: a 5′ deletion of *cutC* that maintains MicL but deletes the first 104 codons of *cutC* (*cutC*Δ5′) and a MicL promoter mutant (point mutations in P_{micL} −10 and −35 motifs) that conserves CutC protein sequence (P_{micL} mutant). Northern analysis confirmed that MicL and MicL-S expression was nearly abolished by P_{micL} mutation (Supplemental Fig. S8B), and Western analysis confirmed that CutC is not synthesized in the *cutC*Δ5′ mutant (Supplemental Fig. S1C). The MicL levels were moderately reduced in *cutC*Δ5′ cells, possibly due to effects on P_{micL} (Supplemental Fig. S8B). However, only the P_{micL} mutant has a copper sensitivity phenotype that closely matches that of Δ*cutC* (Fig. 6A; Supplemental Fig. S9). Furthermore, ectopic expression of either MicL or MicL-S dramatically increased the viability of Δ*cutC* on copper (Fig. 6B) without affecting growth (Supplemental Fig. S8D). MicL overexpression also enhanced copper resistance in wild-type cells (Fig. 6B).

As *lpp* is the sole target of MicL, we tested whether reduced synthesis of Lpp underlies copper resistance. Indeed, a Δ*lpp* strain was slightly more resistant to copper than wild-type cells (Fig. 6A; Supplemental Fig. S9), and overexpression of MicL and MicL-S did not increase the copper resistance of Δ*lpp* mutants (Fig. 6B). Together, these

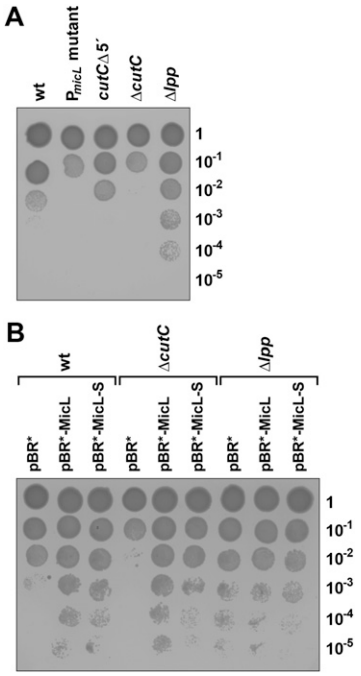

Figure 6. Copper sensitivity of Δ*cutC* is due to loss of MicL. (*A*) Sensitivity of wild-type strains and variants with P_{micL} mutant (-10C-T/-35A-G), *cutC*Δ5′ (which preserves MicL), Δ*cutC*, and Δ*lpp* to 4 mM Cu(II)Cl_2. Three microliters of each strain in exponential phase was spotted on LB supplemented with 4 mM Cu(II)Cl_2 at the indicated dilutions (Tetaz and Luke 1983; Gupta et al. 1995). (*B*) Sensitivity of wild-type cells, Δ*cutC*, and Δ*lpp* transformed with pBR⋆ control vector, pBR⋆-MicL-S, and pBR⋆-MicL to 4 mM Cu(II)Cl_2 using conditions in *A* with the exception that the medium was additionally supplemented with kanamycin. Some differences in sensitivity between *A* and *B* may be due to a synthetic effect between copper and the kanamycin used for plasmid selection in *B*.

data suggest that high levels of Lpp result in copper sensitivity and that MicL confers copper resistance by reducing Lpp levels.

σ^E, MicL, and Lpp form a protective regulatory loop

The essential transcription factor σ^E regulates the folding and levels of abundant membrane proteins such as OMPs. In a previously described regulatory loop (Papenfort et al. 2010; Gogol et al. 2011), σ^E is activated by unfolded OMPs and in turn induces expression of the MicA and RybB sRNAs, which oppose stress by down-regulating OMP mRNAs. MicL and Lpp may constitute another σ^E-dependent regulatory loop that opposes stresses associated with Lpp accumulation. We tested whether the MicL, Lpp, and σ^E relationship was similar to that established for RybB and MicA, OMPs, and σ^E. Indeed, σ^E activity responds to Lpp levels. Although Lpp is already the most abundant protein in the cell, mild overexpression of Lpp (approximately twofold) leads to activation of the σ^E response, and high overexpression (approximately threefold) leads to significant σ^E activity and growth arrest (Fig. 7A; Supplemental Fig. S10A).

Others have found that σ^E activity is inhibited in cells that have lost *lpp* (Mecsas et al. 1993). Similarly, we observed that reducing Lpp levels 10-fold by MicL overexpression leads to a reduction in σ^E activity (Fig. 7B; Supplemental S10B). In addition, Northern analysis showed that cells lacking MicL (Δ*cutC* strain) have ~1.5-fold higher RybB levels in stationary phase (Supplemental Fig. S10C), consistent with higher σ^E activity.

Finally and most importantly, overexpression of MicL is able to rescue the growth defect associated with depletion of σ^E activity (Fig. 7C; Supplemental Fig. S10D; De Las Peñas et al. 1997; Hayden and Ades 2008), as was observed for MicA and RybB overexpression (Papenfort et al. 2010; Gogol et al. 2011). The ~50-fold to 100-fold decrease in viability caused by overexpressing the σ^E negative regulators RseA and RseB is rescued comparably by coexpressing either MicL or MicA (Fig. 7C; Supplemental Fig. S10D). We conclude that MicL and Lpp represent an additional sRNA loop with an OM-protective function similar to the other σ^E-dependent sRNAs.

Discussion

Lpp is the most abundant protein in the cell and is of central importance in OM homeostasis. It is both embedded in the OM and covalently linked to the peptidoglycan layer, forming an important linkage that connects the OM to the rest of the cell. In this study, we established that MicL, a σ^E-dependent sRNA, specifically targets *lpp* mRNA, preventing its translation. We show that *lpp* is the sole MicL target under conditions that we tested. This stands in contrast to most sRNAs, which act via limited base-pairing to regulate multiple targets. Additionally, MicL is transcribed from within the coding region of the gene *cutC*, and we show that it is responsible for all known phenotypes of *cutC*. Our results put σ^E at the center of an sRNA and protein network that monitors lipoprotein biogenesis and regulates the majority of proteins destined for the membrane.

MicL is a dedicated regulator of Lpp

Lpp exists in ~1 million copies per cell (~2% of dry cell weight) (Narita and Tokuda 2010; Li et al. 2014) and comprises ~10% of all cellular mRNA and ~8% of all translation events in our conditions. Loss of Lpp leads to a weakened and less tethered OM, causing increased vesiculation, leakage of periplasmic contents, and sensitivity to a variety of compounds (Hirota et al. 1977; Suzuki et al. 1978). Inappropriate up-regulation of Lpp likewise is deleterious: Defects in Lpp transport or mislocalization of Lpp to the inner membrane leads to cell death (Yakushi et al. 1997). Thus, the levels of this protein must be maintained in a narrow range for optimum growth.

Two unique features of the Lpp life cycle make post-transcriptional regulation by MicL attractive. First, the cell cannot respond to defects in Lpp transport by up-regulating lipoprotein chaperones and transport machines, as these factors use some of the same transport machines

as Lpp (Narita and Tokuda 2010). Second, transcriptional repression will not rapidly lower Lpp flux, since *lpp* mRNA is unusually stable ($T_{1/2}$ ~10 min in vivo) (Nilsson et al. 1984; Ingle and Kushner 1996). MicL repression of Lpp translation elegantly solves both problems: Blocking ribosome initiation on *lpp* decreases Lpp translation and accelerates degradation of *lpp* mRNA to <4 min based on analysis of our mRNA-seq data. Increased degradation is likely the result of both increased access to RNases, resulting from decreased translation, and recruitment of RNase E through its association with Hfq. MicL-mediated regulation has a further advantage because sRNAs continually inhibit their targets. This is likely to generate less variance in mRNA expression than inhibition of transcription (Levine et al. 2007), which can generate bursts in mRNA synthesis when repressors transiently dissociate from DNA (for review, see Eldar and Elowitz 2010).

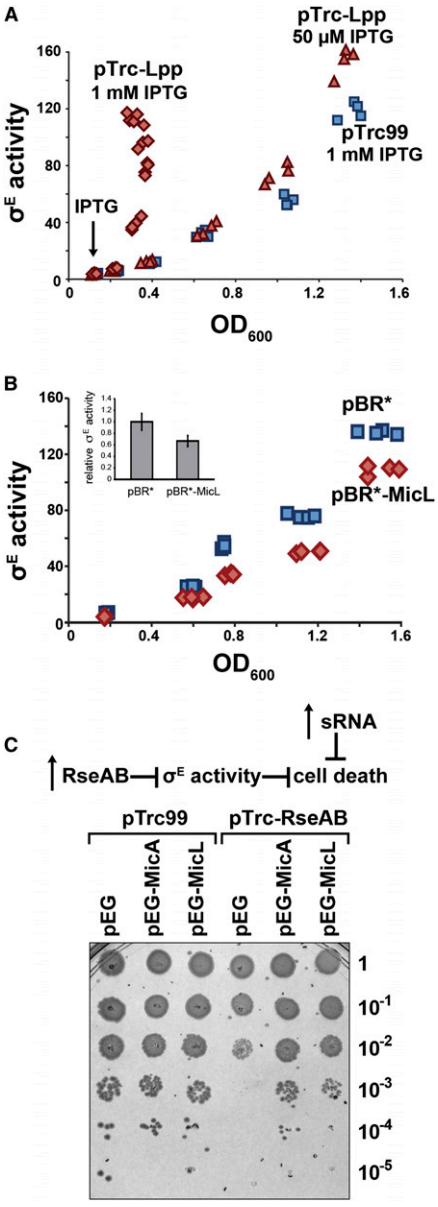

It is notable that MicL has only a single mRNA target. This stands in contrast to all other Hfq-binding sRNA regulators characterized thus far. Lpp might necessitate an sRNA dedicated to controlling the rate of its synthesis due to its enormous abundance. Since *lpp* is in such high excess over other mRNAs, a second target may be difficult to regulate, as competition for base-pairing with MicL could prevent the down-regulation of the less well-expressed transcript (Levine et al. 2007) such that the secondary mRNA targets would not be regulated until most of the *lpp* mRNA is degraded.

σ^E-Regulated sRNAs repress protein synthesis of all of the most abundant OM proteins

Our results place σ^E at the center of an elaborate regulatory system that monitors and responds to defects in all aspects of the OM biogenesis (Fig. 8). σ^E senses OM status through the degradation rate of its negative regulator, RseA, which is mediated by DegS and RseB. DegS and RseB respond, respectively, to misaccumulation of OMPs and LPS. Upon stress, σ^E up-regulates proteins facilitating OMP and LPS assembly and transport. In addition, σ^E up-regulates the MicA and RybB sRNAs to down-regulate OMP synthesis and, as we showed here, MicL to down-regulate Lpp synthesis. The MicA and RybB sRNAs are part of a regulatory loop that opposes stresses associated with OMP folding and assembly. Our data for MicL/Lpp indicate that they constitute a second σ^E-dependent protective regulatory loop to oppose stresses associated with Lpp folding. We suggest that σ^E senses Lpp status as an indirect consequence of monitoring OMP and LPS assembly. The essential lipoprotein components of the OM assembly machines of OMPs (BamD) and LPS (LptE) (for review, see Silhavy et al. 2010) are in direct competition with Lpp, as all lipopro-

Figure 7. MicL and Lpp are part of an envelope protective regulatory loop. (*A*) Overexpression of Lpp increases σ^E activity. Cells with either control vector or pTrc-Lpp were induced with either 50 μM or 1 mM IPTG (at the time indicated). σ^E activity was measured from a σ^E-dependent *rpoHp3-lacZ* reporter. The σ^E activity for the vector control strain treated with 50 μM or 1 mM IPTG was similar at all points (data not shown). (*B*) Overexpression of MicL lowers σ^E activity. Cells with empty vector or pBR*-MicL were induced with 1 mM IPTG when overnight cultures were diluted to OD_{600} ~0.01. σ^E activity was measured as in *A*. Notably, MicL overexpression lowers Lpp protein levels to an extent similar to that observed in ribosome profiling (~10-fold) (cf. Fig. 2C; Supplemental Fig. S10B). The *inset* provides the average and standard deviation for increased σ^E activity for all pBR* and pBR*-MicL points, normalized to pBR* at each time point. (*C*) Shutoff of σ^E activity leads to cell death and can be rescued by concomitant expression of MicA or MicL from derivatives of the pEG plasmid. σ^E activity is shut off by overexpressing the σ^E-negative regulators RseA/B from pTrc-RseAB. Aliquots (2 μL) of cells growing exponentially in LB with ampicillin (amp) and cm were plated at the indicated dilutions on LB plates ± 1 mM IPTG, which induces both RseA/B and the sRNA (MicL or MicA).

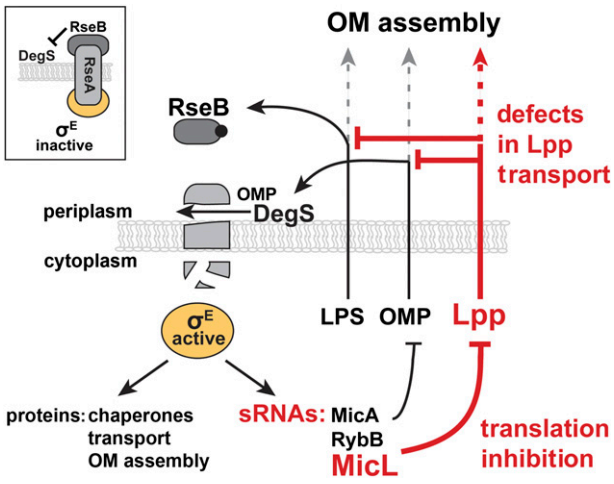

Figure 8. Model of the envelope protective σ^E–MicL–Lpp loop. σ^E transcribes genes encoding proteins that relieve folding stress and sRNAs that inhibit new synthesis of the abundant proteins of the OM (OMPs and Lpp). Defects in lipoprotein transport inhibit proper OM assembly of both LPS and OMPs, which then bind to RseB and DegS, respectively, inducing RseA cleavage and σ^E activation. In response, σ^E activates the sRNA MicL to specifically down-regulate synthesis of Lpp, the major lipoprotein. (*Inset*) σ^E is held inactive by RseA in the inner membrane. RseB binds to RseA and prevents DegS from cleaving RseA.

teins are chaperoned by the LolA/LolB system. Thus, transient overexpression of Lpp will decrease OM insertion of the BamD/LptE lipoproteins and assembly of their respective machines. This will disrupt LPS and OMP insertion into the membrane, triggering the concomitant accumulation of both LPS and OMPs and σ^E activation.

Together, MicL, MicA, and RybB regulate not only the majority of protein flux targeted to the OM (>85% of the translation of OM proteins) but also a large fraction of total cell protein (~12% of all translation events) (Supplemental Table S3). As production of OM proteins consumes a large fraction of the cellular resources (~14% of all transcription and translation is devoted to OM proteins) (Supplemental Table S3), σ^E is the regulator of a large section of cellular physiology. Given the central role of these sRNAs in controlling flux of membrane proteins, it is not surprising that their overexpression relieves cell death resulting from insufficient σ^E. Although physiological levels of these sRNAs do not fully eliminate Lpp or OMP synthesis, they cause a modest decrease in translation, which nonetheless may have a large effect due to the abundance of these proteins. Even a twofold change in the availability of *lpp* mRNA would affect 4% of all translation events and alter the composition the membrane.

During transition to stationary phase, nutrient limitation severely curtails cell growth, requiring a significantly reduced rate of membrane synthesis. Indeed, we observed a dramatic decrease in the levels of the *lpp* and *omp* mRNAs during this condition. The necessity of down-regulating new synthesis of Lpp and OMPs may explain why there is a dramatic rise in σ^E activity and the levels of MicL, RybB, and MicA during this transition. As both *lpp* and *omp* mRNAs are exceptionally long-lived and well translated, up-regulating these sRNAs simultaneously inhibits new synthesis of these proteins and allows RNases to degrade the mRNAs, thereby facilitating adaptation to stationary phase.

Copper sensitivity is related to lipoprotein biogenesis

We found that cells lacking MicL misregulate Lpp and are sensitive to copper stress. Interestingly, defects in other aspects of lipoprotein homeostasis also lead to increased copper sensitivity. Two additional *cut* genes, the OM lipoprotein *nlpE* (*cutF*) and apolipoprotein N-acyltransferase *lnt* (*cutE*) (Gupta et al. 1993), are involved in lipoprotein homeostasis. Lnt is an essential protein that catalyzes lipid attachment to lipoproteins such as Lpp and is the last step in lipoprotein maturation (Narita and Tokuda 2010). Importantly, Δ*lpp* complements the copper sensitivity of partially defective *lnt* alleles (Gupta et al. 1993) as well as Δ*nlpE* and Δ*nlpE* Δ*cutC* (data not shown), suggesting that these copper sensitivity phenotypes reflect Lpp misregulation arising from altered Lpp insertion into the OM or an altered OM environment. Thus, monitoring and controlling Lpp biogenesis is a key component of resistance to copper.

The *cutC* gene received its name because mutations in the coding sequence conferred sensitivity to copper. Since our investigations establish that this phenotype instead derives from misregulation of MicL and consequent alteration of Lpp biogenesis, the function of CutC should be re-examined. However, it is intriguing that CutC and the YecM protein encoded in the same operon have been hypothesized to be metal-binding proteins (Gupta et al. 1995; Zhang et al. 2003b). While there is no direct evidence for copper association with bacterial CutC, the conserved human variant of CutC has been shown to bind Cu(I) (Li et al. 2010). Are the functions of CutC and MicL related and are there advantages of hosting MicL within *cutC*? Since MicL-S can be processed from the *cutC* mRNA (Supplemental Fig. S3F), MicL levels could be tied to *cutC* levels, allowing MicL to be made during exponential phase when σ^E activity is low.

Identification of increasing numbers of 3′ UTR-embedded sRNAs warrants reconsideration of phenotypes attributed to proteins

It is becoming appreciated that sRNAs are not only encoded as independent transcripts in intergenic regions but also originate from within coding regions. sRNAs can be generated by the processing of a larger transcript, as in the case of s-SodF in *Streptomyces coelicolor* (Kim et al. 2014), or transcribed as a primary transcript like MicL (described here) and DapZ in *S. enterica* (Chao et al. 2012). Intriguingly, many of the other candidate 3′ UTR-embedded sRNAs identified in *S. enterica* (Chao et al. 2012) can be observed in our data set. The fact that the majority of these sRNA transcripts are associated with Hfq strongly implies that they are functional (Chao et al. 2012).

Most sRNA discovery efforts have focused on unique transcripts in intergenic regions, but redirected searches to identify further coding region-embedded sRNAs are likely to be worthwhile. With the need for bacteria to rapidly generate novel regulators to fine-tune gene expression, 3′ UTRs are an ideal region of the genome to evolve novel *trans*-encoded sRNA regulators. Since Hfq-binding sRNAs appear to require strong transcription terminators, co-opting existing terminators abrogates the need to evolve this structure de novo. Additionally, the UTRs of genes are the perfect platform for natural selection to search for beneficial mutations in a manner that is less likely to be deleterious. Thus, 3′ UTRs may be a reservoir for evolution and may diversify faster than other parts of the genome.

The question of evolution is also interesting to consider in the case of MicL. σ^E and its protein regulators are broadly conserved among the γ-proteobacteria, and the existing data suggest that the pathways activating σ^E are broadly conserved as well. For example, in *Pseudomonas aeruginosa*, homologs of the σ^E regulators respond to the same OMP peptide sequences and LPS stimuli as in the *E. coli* system (Cezairliyan and Sauer 2009; Lima et al. 2013). Our phylogenetic analysis suggests that MicL, like MicA and RybB, is limited to only a subgroup of γ-proteobacteria (Johansen et al. 2006; Papenfort et al. 2006), but sRNAs whose expression is σ^E-dependent have been reported for other bacteria in this phylum (Park et al. 2014). Some of these σ^E-dependent sRNAs may fulfill a role similar to *E. coli* MicA, RybB, and MicL. Alternatively, MicL, MicA, and RybB could have evolved in response to a particular lifestyle of enteric bacteria. Since the major factors of the OM (OMPs, LPS, and Lpp) are recognized by the host immune system (for review, see Galdiero et al. 2012), regulating their levels with sRNAs could be an adaptation to evade detection.

Our study of MicL indicates that investigations of sRNA function continue to provide fundamental insights into bacterial cell physiology. We suggest that additional sRNAs important to cellular physiology are masked in protein-coding regions and that existing phenotypes associated with protein products may be misattributed and instead arise from misregulation of sRNAs.

Materials and methods

Strains and plasmids

The bacterial strains and plasmids used in the study are listed in Supplemental Tables S4 and S5, respectively. Gene knockouts or mutants were constructed in strain NM500 or NM400 using λ Red-mediated recombination with DNA fragments generated by PCR using oligonucleotides listed in Supplemental Table S6 (Datsenko and Wanner 2000; Yu et al. 2000; Court et al. 2003). The mutations linked to markers flanked by FRT sites were moved into new backgrounds by P1 transduction, and, where indicated, antibiotic resistance markers were removed using plasmid pCP20 (Cherepanov and Wackernagel 1995). For the *lpp-lacZ* translational fusions (and mutant derivatives), the entire 5′ UTR, beginning with the major *lpp* transcription start at position 1,755,407 to the indicated position in the coding sequence, was fused to the coding sequence of *lacZ* behind a P_{BAD} promoter (Mandin and Gottesman 2009). A second *lpp* promoter was annotated in EcoCyc at position 1,755,320, but only a very weak signal was detected in our deep sequencing analysis (MK Thomason, T Bischler, SK Eisenbart, KU Förstner, A Zhang, A Herbig, K Nieselt, CM Sharma, G Storz, in prep.). In all cases, point mutations were introduced in the fragments used for recombination using overlapping PCR as described previously (Ho et al. 1989).

For plasmid construction, the desired gene fragments were generated by PCR amplification using MG1655 genomic DNA as a template and, after digestion with restriction enzymes, were cloned into the corresponding sites of the indicated vectors. pBR⋆ is a derivative of the pBR322-derived pBRplac vector (here denoted as pBR) (Guillier and Gottesman 2006) in which the ampicillin cassette was replaced by the kanamycin cassette. pBR′ contains both the ampicillin and the kanamycin cassettes. We found transforming with pBR⋆-MicL to be more efficient than transforming with pBR-MicL, possibly due to the effects of kanamycin versus ampicillin. All cloning was performed using *E. coli* TOP10 cells (Invitrogen), and all mutations and plasmid inserts were confirmed by sequencing.

Growth conditions

Unless indicated otherwise, strains were grown aerobically at 37°C in either LB (10 g of tryptone, 5 g of yeast extract, 10 g of NaCl per liter) or EZ rich defined medium (MOPS, Teknova). The copper sensitivity was monitored on LB plates supplemented with 4 mM $Cu(II)Cl_2$ (diluted from 1 M stock solution; Sigma) and incubated overnight at 30°C (Tetaz and Luke 1983; Gupta et al. 1995). Where indicated, IPTG was added at a final concentration of 1 mM or as noted, and antibiotics and chemicals were added when appropriate at the following concentrations: 100 μg mL^{-1} ampicillin, 30 μg mL^{-1} kanamycin, 12.5 μg mL^{-1} tetracycline, 25 μg mL^{-1} chloramphenicol, or 1.4 mM dibucaine.

Tiling array analysis

Cultures of *E. coli* carrying the σ^E overexpression plasmid (pRpoE) were grown to OD_{600} ~0.3 at 30°C in LB, and pre-induction (0 min) and post-induction (20 min) samples were harvested. After RNA extraction with hot phenol chloroform as described (Massé et al. 2003), each sample was hybridized to a custom Affymetrix *E. coli* tiling array, and an antibody specific for RNA–DNA complexes detected "ON" tiles as described (Hu et al. 2006). The tiling array tools provided by Affymetrix, tiling analysis software (TAS) and the integrated genome browser (IGB), were used to analyze the data set.

Deep sequencing and analysis

mRNA-seq and ribosome profiling were performed as previously described, with a few modifications (Ingolia et al. 2009; Li et al. 2012). Briefly, cells were grown in MOPS to OD ~0.3 and induced with 1 mM IPTG; at the indicated times, 200 mL of cells was harvested. Two replicates were performed for all MicL experiments, with high levels of correlation between experiments. For RNA-seq, the cell pellet was phenol-extracted, and ribosomal RNA was removed with the MICROBExpress kit (Life Technologies). tRNAs were not removed to recover the small RNAs of the cell. For ribosome profiling, ribosome-protected fragments were generated as previously described, yielding 25- to 40-nt footprints (Ingolia et al. 2009; Oh et al. 2011). rRNA was removed, samples were converted to a sequencing library (Ingolia et al. 2009; Li et al. 2012), and sequencing was performed

on an Illumina HiSeq 2000 and aligned to NC_000913.fna (MG1655), allowing for one mismatch.

Analysis was restricted to genes with >128 total counts, a cutoff determined empirically to prevent false positives (Ingolia et al. 2009). Mean mRNA density and ribosome density were calculated excluding the 5′ and 3′ UTRs and were corrected for total number of reads and the length of each gene and reported in reads per kilobase per million (RPKM) (Ingolia et al. 2009). Translation efficiency was calculated on a gene-by-gene basis, where translation efficiency was the ratio of ribosome footprints to mRNA fragments for that gene (mean translation/mean expression) (Ingolia et al. 2009). To calculate each fraction of the total mRNA and translation that each protein represents, the total number of reads per coding region was divided by the total number of reads across all coding regions. All of the deep sequencing data sets are available at Gene Expression Omnibus (GSE58637).

Northern analysis

For Northern analysis, total RNA was extracted by hot acid phenol as described previously (Massé et al. 2003), with minor modifications. Briefly, cells in 1.5 mL of culture (the equivalent of OD_{600} ~3) were collected, resuspended in 650 µL of buffer A (0.5% SDS, 20 mM NaOAc, 10 mM EDTA), and immediately added to 750 µL of hot acid phenol chloroform (pH 4.5; Ambion). The mixture was vortexed vigorously and incubated for 10 min at 65°C. The sample was then centrifuged at 30,000 rpm for 10 min, and the upper aqueous phase was subjected to another round of hot acid phenol chloroform treatment. The aqueous phase from the second acid phenol extraction was added to a Phase Lock Gel Heavy 2.0-mL tube (5Prime) containing 1 mL of phenol chloroform (pH 8; Invitrogen) and mixed and spun at 30,000 rpm for 10 min at 4°C. The supernatant was combined with 1 mL of 100% ethanol containing 1 µL of 20 mg/mL glycogen and precipitated at −80°C. The RNA was collected by centrifugation at 30,000 rpm for 30 min at 4°C, washed twice with 1 mL of 70% ethanol, air-dried, and resuspended in nuclease-free dH_2O. Total RNA concentration was determined based on OD_{260}.

Northern blots were performed as previously described (Thomason et al. 2012) with minor modifications. Briefly, 10 µg of total RNA was separated on an 8% polyacrylamide–7 M urea gel (USB Corporation) in 1× TBE and transferred to Zeta-Prove membrane (Bio-Rad) overnight at 20 V in 0.5× TBE. Oligonucleotides were end-labeled with γ-^{32}P-ATP by T4 polynucleotide kinase (New England Biolabs). Membranes were UV cross-linked and hybridized overnight at 45°C in UltraHyb (Ambion) hybridization buffer. Following hybridization, membranes were washed once with 2× SSC + 0.1% SDS followed by a 10-min incubation at 45°C with 2× SSC + 0.1% SDS. Membranes were subsequently washed five times with 0.2× SSC + 0.1% SDS, allowed to air dry for 5 min, and exposed to KODAK Biomax X-ray film at −80°C.

Hfq coimmunoprecipitation

Hfq coimmunoprecipitation was carried out as described (Zhang et al. 2003a). Briefly, cells in 15 mL of wild-type or Δ*hfq-1::cm* cultures grown to late stationary phase (~14 h) were pelleted, resuspended in 400 µL of lysis buffer (20 mM Tris-HCl at pH 8.0, 150 mM KCl, 1 mM $MgCl_2$, 1 mM DTT, 0.2 U RNaseOUT [Ambion]), and lysed by vortexing with ~0.6 g of glass beads for 10 min. To immunoprecipitate Hfq, 200 µL of cell lysate was combined with 24 mg of protein A Sepharose CL-4B beads (Amersham Biosciences) complexed with 20 µL of α-Hfq serum, 200 µL of Net2 buffer (50 mM Tris-HCl at pH 7.4, 150 mM NaCl, 0.05% Triton X-100), and 1 µL of RNaseOUT. The mixture was incubated for 2 h at 4°C with rotation then washed five times with 1.5 mL of Net2 buffer. Following the washes, the beads were extracted with 400 µL of Net2 buffer, 50 µL of 3 M NaOAc, 5 µL of 10% SDS, and 600 µL of phenol:chloroform:isoamyl alcohol (Ambion), and RNA was ethanol-precipitated. Total RNA was isolated by Trizol (Invitrogen) extraction followed by chloroform extraction and ethanol precipitation. Total RNA (5 µg) or coimmunoprecipitated RNA (0.5 µg) was then subjected to Northern analysis as described above.

Immunoblot analysis

Western blot analysis was performed as described previously with minor changes (Beisel and Storz 2011; Thomason et al. 2012). Samples were separated on a precasted 5%–20% Tris-Glycine (Bio-Rad) or 16% Tris-Tricine (Invitrogen) and transferred to a nitrocellulose membrane (Invitrogen). Membranes were blocked in 5% milk. To detect Lpp, the blocked membranes were probed with a 1:100,000 dilution of α-Lpp antibody (kindly provided by the laboratory of T. Silhavy) followed by incubation with a 1:20,000 dilution of HRP goat anti-rabbit IgG (Abcam) or a 1:10,000 dilution of IRDye800 goat anti-rabbit IgG (Licor). To detect GroEL, the membranes were incubated with a 1:20,000 dilution of α-GroEL mouse monoclonal (Abcam) followed by incubation with a 1:40,000 dilution of HRP goat anti-mouse IgG (Abcam). For both Lpp and GroEL, the membranes were developed using SuperSignal West Pico chemiluminescent substrate (Thermo Scientific) and exposed to KODAK Blue-XB film. To detect RpoA, the membranes were incubated with a 1:1000 dilution of α-RpoA mouse monoclonal antibody (Neoclone) followed by incubation with 1:10,000 IRDye680 goat anti-mouse IgG (Licor). Fluorescent antibodies were visualized on an Odyessy imager (Licor).

β-Galactosidase assays

β-Galactosidase assays were performed as described previously (Beisel et al. 2012), with some minor modifications. Briefly, four separate colonies were grown overnight in LB with appropriate antibiotics, diluted 1:200 to OD_{600} ~0.03 in the same medium supplemented with 1 mM IPTG and 0.02% L-arabinose, and grown to final OD_{600} = ~1 at 37°C. Five microliters of cells was lysed in 700 µL of Z buffer with 15 µL of 0.1% SDS and 30 µL of chloroform. The OD_{600} and A_{420} of the cultures were measured using an Ultrospec 3300 UV/Vis spectrophotometer (Pharmacia Biotech).

For σ^E activity assays, β-galactosidase activity was measured from an *rpoHp3*-LacZ reporter as described previously (Ades et al. 1999; Costanzo and Ades 2006). Briefly, cells were grown to OD_{600} ~0.1 in LB at 30°C. Four samples were taken at different times, and the β-galactosidase activities of these samples were plotted against their OD_{600}. The slope of this plot represents σ^E activity. Four independent experiments were performed for each strain. For Figure 7B, a mean and standard deviation of pMicL to pBR* were calculated at each time point and aggregated across all time points.

Promoter activity assays

The MicL promoter-GFP fusion was constructed as described previously (Mutalik et al. 2009), placing the P_{micL} −65 to +20 sequences in front of GFP. Other promoter-GFP fusions are from

Mutalik et al. (2009). GFP fluorescence was measured using a Varioskan (Thermo) as previously described (Mutalik et al. 2009). Briefly, promoter strength is a function of the fluorescence and the cell density. GFP fluorescence was measured at four ODs after σ^E induction, and the fluorescence was plotted versus OD. The slope of the linear portion of this plot is reported as the promoter activity of the specific promoter-GFP fusion in that reporter strain.

Acknowledgments

We thank A. Zhang for assistance with the tiling array analysis, S. Gottesman for plasmids and strains, T. Silhavy for sharing Lpp antiserum, and G.-W. Li and D. Burkhardt for helpful discussions. Work in the Gross laboratory was supported by National Institute of General Medical Science (GM036278), and work in the Storz laboratory was supported by the Intramural Research Program of the Eunice Kennedy Shriver National Institute of Child Health and Human Development (ZIA HD001608-23). This work was also supported by the Intramural Research Program of the National Library of Medicine.

References

Ades SE, Connolly LE, Alba BM, Gross CA. 1999. The *Escherichia coli* σ^E-dependent extracytoplasmic stress response is controlled by the regulated proteolysis of an anti-σ factor. *Genes Dev* **13:** 2449–2461.

Barchinger SE, Ades SE. 2013. Regulated proteolysis: control of the *Escherichia coli* σ^E-dependent cell envelope stress response. *Subcell Biochem* **66:** 129–160.

Beisel CL, Storz G. 2011. The base-pairing RNA Spot 42 participates in a multioutput feedforward loop to help enact catabolite repression in *Escherichia coli*. *Mol Cell* **41:** 286–297.

Beisel CL, Updegrove TB, Janson BJ, Storz G. 2012. Multiple factors dictate target selection by Hfq-binding small RNAs. *EMBO J* **31:** 1961–1974.

Bouvier M, Sharma CM, Mika F, Nierhaus KH, Vogel J. 2008. Small RNA binding to 5′ mRNA coding region inhibits translational initiation. *Mol Cell* **32:** 827–837.

Braun V, Rehn K. 1969. Chemical characterization, spatial distribution and function of a lipoprotein (murein-lipoprotein) of the *E. coli* cell wall. The specific effect of trypsin on the membrane structure. *Eur J Biochem* **10:** 426–438.

Braun M, Silhavy TJ. 2002. Imp/OstA is required for cell envelope biogenesis in *Escherichia coli*. *Mol Microbiol* **45:** 1289–1302.

Cezairliyan BO, Sauer RT. 2009. Control of *Pseudomonas aeruginosa* AlgW protease cleavage of MucA by peptide signals and MucB. *Mol Microbiol* **72:** 368–379.

Chaba R, Grigorova IL, Flynn JM, Baker TA, Gross CA. 2007. Design principles of the proteolytic cascade governing the σ^E-mediated envelope stress response in *Escherichia coli*: keys to graded, buffered, and rapid signal transduction. *Genes Dev* **21:** 124–136.

Chaba R, Alba BM, Guo MS, Sohn J, Ahuja N, Sauer RT, Gross CA. 2011. Signal integration by DegS and RseB governs the σ^E-mediated envelope stress response in *Escherichia coli*. *Proc Natl Acad Sci* **108:** 106–111.

Chang TW, Lin YM, Wang CF, Liao YD. 2012. Outer membrane lipoprotein Lpp is Gram-negative bacterial cell surface receptor for cationic antimicrobial peptides. *J Biol Chem* **287:** 418–428.

Chao Y, Papenfort K, Reinhardt R, Sharma CM, Vogel J. 2012. An atlas of Hfq-bound transcripts reveals 3′ UTRs as a genomic reservoir of regulatory small RNAs. *EMBO J* **31:** 4005–4019.

Cherepanov PP, Wackernagel W. 1995. Gene disruption in *Escherichia coli*: TcR and KmR cassettes with the option of Flp-catalyzed excision of the antibiotic-resistance determinant. *Gene* **158:** 9–14.

Coornaert A, Lu A, Mandin P, Springer M, Gottesman S, Guillier M. 2010. MicA sRNA links the PhoP regulon to cell envelope stress. *Mol Microbiol* **76:** 467–479.

Costanzo A, Ades SE. 2006. Growth phase-dependent regulation of the extracytoplasmic stress factor, σ^E, by guanosine 3′,5′-bispyrophosphate (ppGpp). *J Bacteriol* **188:** 4627–4634.

Court DL, Swaminathan S, Yu D, Wilson H, Baker T, Bubunenko M, Sawitzke J, Sharan SK. 2003. Mini-λ: a tractable system for chromosome and BAC engineering. *Gene* **315:** 63–69.

Cowles CE, Li Y, Semmelhack MF, Cristea IM, Silhavy TJ. 2011. The free and bound forms of Lpp occupy distinct subcellular locations in *Escherichia coli*. *Mol Microbiol* **79:** 1168–1181.

Datsenko KA, Wanner BL. 2000. One-step inactivation of chromosomal genes in *Escherichia coli* K-12 using PCR products. *Proc Natl Acad Sci* **97:** 6640–6645.

De Las Peñas A, Connolly LE, Gross CA. 1997. σ^E is an essential σ factor in *Escherichia coli*. *J Bacteriol* **179:** 6862–6864.

Desnoyers G, Bouchard MP, Massé E. 2013. New insights into small RNA-dependent translational regulation in prokaryotes. *Trends Genet* **29:** 92–98.

Eldar A, Elowitz MB. 2010. Functional roles for noise in genetic circuits. *Nature* **467:** 167–173.

Galdiero S, Falanga A, Cantisani M, Tarallo R, Della Pepa ME, D'Oriano V, Galdiero M. 2012. Microbe-host interactions: structure and role of Gram-negative bacterial porins. *Curr Protein Pept Sci* **13:** 843–854.

Gogol EB, Rhodius VA, Papenfort K, Vogel J, Gross CA. 2011. Small RNAs endow a transcriptional activator with essential repressor functions for single-tier control of a global stress regulon. *Proc Natl Acad Sci* **108:** 12875–12880.

Guillier M, Gottesman S. 2006. Remodelling of the *Escherichia coli* outer membrane by two small regulatory RNAs. *Mol Microbiol* **59:** 231–237.

Guisbert E, Rhodius VA, Ahuja N, Witkin E, Gross CA. 2007. Hfq modulates the σ^E-mediated envelope stress response and the σ^{32}-mediated cytoplasmic stress response in *Escherichia coli*. *J Bacteriol* **189:** 1963–1973.

Gupta SD, Gan K, Schmid MB, Wu HC. 1993. Characterization of a temperature-sensitive mutant of *Salmonella typhimurium* defective in apolipoprotein N-acyltransferase. *J Biol Chem* **268:** 16551–16556.

Gupta SD, Lee BT, Camakaris J, Wu HC. 1995. Identification of *cutC* and *cutF* (*nlpE*) genes involved in copper tolerance in *Escherichia coli*. *J Bacteriol* **177:** 4207–4215.

Hayden JD, and Ades SE (2008). The extracytoplasmic stress factor,σE, is required to maintain cell envelope integrity in Escherichia coli. PLoS ONE **3:** e1573.

Hirota Y, Suzuki H, Nishimura Y, Yasuda S. 1977. On the process of cellular division in *Escherichia coli*: a mutant of *E. coli* lacking a murein-lipoprotein. *Proc Natl Acad Sci* **74:** 1417–1420.

Ho SN, Hunt HD, Horton RM, Pullen JK, Pease LR. 1989. Site-directed mutagenesis by overlap extension using the polymerase chain reaction. *Gene* **77:** 51–59.

Hu Z, Zhang A, Storz G, Gottesman S, Leppla SH. 2006. An antibody-based microarray assay for small RNA detection. *Nucleic Acids Res* **34:** e52.

Ingle CA, Kushner SR. 1996. Development of an in vitro mRNA decay system for *Escherichia coli*: poly(A) polymerase I is necessary to trigger degradation. *Proc Natl Acad Sci* **93:** 12926–12931.

Ingolia NT, Ghaemmaghami S, Newman JRS, Weissman JS. 2009. Genome-wide analysis in vivo of translation with nucleotide resolution using ribosome profiling. *Science* **324:** 218–223.

Inouye M, Shaw J, Shen C. 1972. The assembly of a structural lipoprotein in the envelope of *Escherichia coli*. *J Biol Chem* **247:** 8154–8159.

Johansen J, Rasmussen AA, Overgaard M, Valentin-Hansen P. 2006. Conserved small non-coding RNAs that belong to the σ^E regulon: role in down-regulation of outer membrane proteins. *J Mol Biol* **364:** 1–8.

Johansen J, Eriksen M, Kallipolitis B, Valentin-Hansen P. 2008. Down-regulation of outer membrane proteins by noncoding RNAs: unraveling the cAMP-CRP- and σ^E-dependent CyaR-*ompX* regulatory case. *J Mol Biol* **383:** 1–9.

Kim HM, Shin JH, Cho YB, Roe JH. 2014. Inverse regulation of Fe- and Ni-containing SOD genes by a Fur family regulator Nur through small RNA processed from 3′UTR of the *sodF* mRNA. *Nucleic Acids Res* **42:** 2003–2014.

Levine E, Zhang Z, Kuhlman T, Hwa T. 2007. Quantitative characteristics of gene regulation by small RNA. *PLoS Biol* **5:** e229.

Li Y, Du J, Zhang P, Ding J. 2010. Crystal structure of human copper homeostasis protein CutC reveals a potential copper-binding site. *J Struct Biol* **169:** 399–405.

Li G-W, Oh E, Weissman JS. 2012. The anti-Shine-Dalgarno sequence drives translational pausing and codon choice in bacteria. *Nature* **484:** 538–541.

Li G-W, Burkhardt DH, Gross CA, Weissman JS. 2014. Quantifying absolute protein synthesis rates reveals principles underlying allocation of cellular resources. *Cell* **157:** 624–635.

Lima S, Guo MS, Chaba R, Gross CA, Sauer RT. 2013. Dual molecular signals mediate the bacterial response to outer-membrane stress. *Science* **340:** 837–841.

Mandin P, Gottesman S. 2009. A genetic approach for finding small RNAs regulators of genes of interest identifies RybC as regulating the DpiA/DpiB two-component system. *Mol Microbiol* **72:** 551–565.

Massé E, Escorcia FE, Gottesman S. 2003. Coupled degradation of a small regulatory RNA and its mRNA targets in *Escherichia coli*. *Genes Dev* **17:** 2374–2383.

Matveeva O, Nechipurenko Y, Rossi L, Moore B, Saetrom P, Ogurtsov AY, Atkins JF, Shabalina SA. 2007. Comparison of approaches for rational siRNA design leading to a new efficient and transparent method. *Nucleic Acids Res* **35:** e63.

Mecsas J, Rouviere PE, Erickson JW, Donohue TJ, Gross CA. 1993. The activity of σ^E, an *Escherichia coli* heat-inducible σ-factor, is modulated by expression of outer membrane proteins. *Genes Dev* **7:** 2618–2628.

Mizuno T, Chou MY, Inouye M. 1984. A unique mechanism regulating gene expression: translational inhibition by a complementary RNA transcript (micRNA). *Proc Natl Acad Sci* **81:** 1966–1970.

Mutalik VK, Nonaka G, Ades SE, Rhodius VA, Gross CA. 2009. Promoter strength properties of the complete σ E regulon of *Escherichia coli* and *Salmonella enterica*. *J Bacteriol* **191:** 7279–7287.

Narita S, Tokuda H. 2010. Biogenesis and membrane targeting of lipoproteins. *EcoSal Plus* doi: 10.1128/ecosalplus.4.3.7.

Nichols RJ, Sen S, Choo YJ, Beltrao P, Zietek M, Chaba R, Lee S, Kazmierczak KM, Lee KJ, Wong A, et al. 2011. Phenotypic landscape of a bacterial cell. *Cell* **144:** 143–156.

Nikaido H. 2003. Molecular basis of bacterial outer membrane permeability revisited. *Microbiol Mol Biol Rev* **67:** 593–656.

Nilsson G, Belasco JG, Cohen SN, von Gabain A. 1984. Growth-rate dependent regulation of mRNA stability in *Escherichia coli*. *Nature* **312:** 75–77.

Oh E, Becker AH, Sandikci A, Huber D, Chaba R, Gloge F, Nichols RJ, Typas A, Gross CA, Kramer G, et al. 2011. Selective ribosome profiling reveals the cotranslational chaperone action of trigger factor in vivo. *Cell* **147:** 1295–1308.

Opdyke JA, Fozo EM, Hemm MR, Storz G. 2011. RNase III participates in GadY-dependent cleavage of the *gadX–gadW* mRNA. *J Mol Biol* **406:** 29–43.

Papenfort K, Pfeiffer V, Mika F, Lucchini S, Hinton JC, Vogel J. 2006. σ^E-Dependent small RNAs of *Salmonella* respond to membrane stress by accelerating global omp mRNA decay. *Mol Microbiol* **62:** 1674–1688.

Papenfort K, Bouvier M, Mika F, Sharma CM, Vogel J. 2010. Evidence for an autonomous 5′ target recognition domain in an Hfq-associated small RNA. *Proc Natl Acad Sci* **107:** 20435–20440.

Park SH, Bao Z, Butcher BG, D'Amico K, Xu Y, Stodghill P, Schneider DJ, Cartinhour S, Filiatrault MJ. 2014. Analysis of the small RNA *spf* in the plant pathogen *Pseudomonas syringae* pv. *tomato* strain DC3000. *Microbiology* **160:** 941–953.

Rasmussen AA, Eriksen M, Gilany K, Udesen C, Franch T, Petersen C, Valentin-Hansen P. 2005. Regulation of *ompA* mRNA stability: the role of a small regulatory RNA in growth phase-dependent control. *Mol Microbiol* **58:** 1421–1429.

Rhodius VA, Suh WC, Nonaka G, West J, Gross CA. 2006. Conserved and variable functions of the σ^E stress response in related genomes. *PLoS Biol* **4:** e2.

Rhodius VA, Mutalik VK, Gross CA. 2012. Predicting the strength of UP-elements and full-length *E. coli* σ^E promoters. *Nucleic Acids Res* **40:** 2907–2924.

Ricci DP, Silhavy TJ. 2012. The Bam machine: a molecular cooper. *Biochim Biophys Acta* **1818:** 1067–1084.

Richards GR, Vanderpool CK. 2011. Molecular call and response: the physiology of bacterial small RNAs. *Biochim Biophys Acta* **1809:** 525–531.

Silhavy TJ, Kahne D, Walker S. 2010. The bacterial cell envelope. *Cold Spring Harb Perspect Biol* **2:** a000414.

Skovierova H, Rowley G, Rezuchova B, Homerova D, Lewis C, Roberts M, Kormanec J. 2006. Identification of the σ^E regulon of *Salmonella enterica* serovar Typhimurium. *Microbiology* **152:** 1347–1359.

Storz G, Vogel J, Wassarman KM. 2011. Regulation by small RNAs in bacteria: expanding frontiers. *Mol Cell* **43:** 880–891.

Suzuki H, Nishimura Y, Yasuda S, Nishimura A, Yamada M, Hirota Y. 1978. Murein-lipoprotein of *Escherichia coli:* a protein involved in the stabilization of bacterial cell envelope. *Mol Gen Genet* **167:** 1–9.

Tetaz TJ, Luke RK. 1983. Plasmid-controlled resistance to copper in *Escherichia coli*. *J Bacteriol* **154:** 1263–1268.

Thomason MK, Fontaine F, De Lay N, Storz G. 2012. A small RNA that regulates motility and biofilm formation in response to changes in nutrient availability in *Escherichia coli*. *Mol Microbiol* **84:** 17–35.

Thompson KM, Rhodius VA, Gottesman S. 2007. σ^E regulates and is regulated by a small RNA in *Escherichia coli*. *J Bacteriol* **189:** 4243–4256.

Udekwu KI, Wagner EGH. 2007. σ^E Controls biogenesis of the antisense RNA MicA. *Nucleic Acids Res* **35:** 1279–1288.

Udekwu KI, Darfeuille F, Vogel J, Reimegård J, Holmqvist E, Wagner EGH. 2005. Hfq-dependent regulation of OmpA

synthesis is mediated by an antisense RNA. *Genes Dev* **19:** 2355–2366.
Vogel J, Luisi BF. 2011. Hfq and its constellation of RNA. *Nat Rev Microbiol* **9:** 578–589.
Walsh NP, Alba BM, Bose B, Gross CA, Sauer RT. 2003. OMP peptide signals initiate the envelope-stress response by activating DegS protease via relief of inhibition mediated by its PDZ domain. *Cell* **113:** 61–71.
Wu T, Malinverni J, Ruiz N, Kim S, Silhavy TJ, Kahne D. 2005. Identification of a multicomponent complex required for outer membrane biogenesis in *Escherichia coli*. *Cell* **121:** 235–245.
Yakushi T, Tajima T, Matsuyama S, Tokuda H. 1997. Lethality of the covalent linkage between mislocalized major outer membrane lipoprotein and the peptidoglycan of *Escherichia coli*. *J Bacteriol* **179:** 2857–2862.
Yu D, Ellis HM, Lee EC, Jenkins NA, Copeland NG, Court DL. 2000. An efficient recombination system for chromosome engineering in *Escherichia coli*. *Proc Natl Acad Sci* **97:** 5978–5983.
Zhang A, Wassarman KM, Rosenow C, Tjaden BC, Storz G, Gottesman S. 2003a. Global analysis of small RNA and mRNA targets of Hfq. *Mol Microbiol* **50:** 1111–1124.
Zhang RG, Duke N, Laskowski R, Evdokimova E, Skarina T, Edwards A, Joachimiak A, Savchenko A. 2003b. Conserved protein YecM from *Escherichia coli* shows structural homology to metal-binding isomerases and oxygenases. *Proteins* **51:** 311–314.
Zhang G, Meredith TC, Kahne D. 2013. On the essentiality of lipopolysaccharide to Gram-negative bacteria. *Curr Opin Microbiol* **16:** 779–785.